Chapter 4

CONTINUOUS-WAVE SQUARE-WAVE (CWSW) SIGNAL GENERATION AND PEAK INTENSITY ENHANCEMENT (PIE) ANALYSIS

While phase modulation of an optical wave does not affect its amplitude, the combination of phase modulation and filtering can result in amplitude modulation [134]. In addition to narrowing the signal bandwidth, filtering generally results in phase-to-amplitude conversion. This observation prompts one to ask whether it is possible to subject a constant amplitude CW signal to phase modulation and filtering so as to generate an RZ pulse train suitable for transmission. This leads to the discovery that an RZ pulse train can be generated by square-wave phase modulation and filtering the continuous-wave (CW) signal. The signal format that utilizes this RZ pulse train is called continuous-wave square-wave (CWSW). The advantage of this technique is that the shape of an RZ pulse generated from this technique is suitable for transmission in a dispersive medium. Generally, as a pulse propagates along a dispersive medium, such as an optical fiber, it is broadened due to the effect of dispersion, and its peak decreases. This is not true for all pulse shapes, however. In some special cases, the pulse is broadened by the dispersion as usual; however, its peak initially increases and then decreases during propagation. We term this phenomenon peak intensity enhancement (PIE). The RZ pulse generated from our proposed technique exhibits this phenomenon. In addition, the phase characteristic of the CWSW signal resembles that of the SWM signal. That is, the signs of adjacent pulses alternate, which in effect makes the CWSW signal robust to the intrachannel and interchannel impairments, similar to the SWM signal.

This chapter is devoted to discussion of the implementation of the CWSW signal format, and theoretical analysis of its performance in special cases. (More general and complete simulation of system performance of CWSW is contained in Chapter 5 and Chapter 6.) The first section of this chapter covers the generation of an RZ pulse train by

square-wave phase modulation and filtering on a CW signal. The remaining sections are the theoretical analysis of the peak intensity enhancement (PIE). The mathematical model used in the PIE analysis is provided in Section 4.2. It is then followed in Section 4.3 by determination of the threshold in pulse parameters at which the PIE can occur. The physical explanation of the PIE is provided in Section 4.5, and discussions of how pulse parameters affect the PIE is provided in Section 4.6. The spectral characteristic of the pulse used in the PIE analysis is discussed in Section 4.7.

4.1 CW TO RZ PULSE TRAIN CONVERSION BY SQUARE-WAVE PHASE MODULATION AND FILTERING

One may notice from the previous chapter that an alternate-sign RZ pulse train can be generated from a CW laser by employing a SWM modulator. However, the drawback of this technique is that the push-pull type MZ modulator configured as the SWM modulator requires in practice two opposite-sign (180° out-of-phase) sinusoidal clock signals, each driving one arm of the MZ modulator, which is a lithium niobate ($LiNbO_3$) phase modulator [108]. Hence, two separate electrical amplifiers are required, one for each driving signal. For an ideal push-pull type MZ modulator, two driving signals must have the same amplitude to yield an alternate-sign RZ pulse train with no frequency chirp [135]. However, for a practical MZ modulator both arms are not identical; hence, the amplitudes of both driving signals have to be optimally adjusted to minimize the residual chirp [136]. This increases the system complexity even without considering the need of two separate amplifiers for the driving signals. In our approach, a single lithium niobate ($LiNbO_3$) phase modulator and an optical filter are required for the generation of alternate-sign RZ pulse train. Since a phase modulator needs only one amplifier to adjust the amplitude of the driving signal, and the passive optical filter does not require a power supply, system complexity is reduced.

The schematic diagram of the transmitter for the CWSW signal is shown in Fig. 4.1. The phase modulator is driven by a periodic square-wave electrical signal adjusted so that the CW output signal from a CW laser is phase-modulated by a square wave phase function having a frequency of half the bit rate and amplitude of $\pi/2$. This in effect

removes the original carrier component and generates sidebands at odd multiples of half the bit rate from the original carrier frequency. A bandpass optical filter following the phase modulator performs phase-to-amplitude conversion, which results in the generation of an alternate-sign RZ pulse train at the filter output. In terms of the baseband-equivalent mathematical model, the signal at the phase modulator output can be written as

$$q_{nf}(\tau_n) = \sqrt{P_0}\, e^{j\phi(\tau_n)}, \tag{4.1}$$

where P_0 is the peak output power of the CW laser, τ_n is the physical time normalized by the bit period ($\tau_n = \tau / T_b$), and $\phi(\tau_n)$ is the square-wave phase variation having normalized frequency of 1/2 (normalized by the bit rate R_b), and peak amplitude (modulation index) of B. Note that the subscript *nf* means that the effect of filtering has not yet been applied to the signal. Mathematically, $\phi(\tau_n)$ can be written as

$$\phi(\tau_n) = B \sum_{k=-\infty}^{\infty} (-1)^k \Pi(\tau_n - k), \tag{4.2}$$

where $\Pi(\tau_n)$ is a rectangular pulse defined as

$$\Pi(\tau_n) = \begin{cases} 1 & , \quad |\tau_n| \le \dfrac{1}{2} \\ 0 & , \quad |\tau_n| > \dfrac{1}{2} \end{cases}. \tag{4.3}$$

Since the magnitude of $q_{nf}(\tau_n)$ is constant, and its phase is periodic in time with normalized period equal to 2, $q_{nf}(\tau_n)$ given by (4.1) can be expressed in terms of the complex Fourier series as

$$q_{nf}(\tau_n) = \sum_{k=-\infty}^{+\infty} c_k e^{j\pi k \tau_n}, \tag{4.4}$$

where c_k is the complex Fourier series coefficient, which can be evaluated from

$$c_k = \frac{1}{2} \int_a^{a+2} q_{nf}(\tau_n) e^{-j\pi k \tau_n} d\tau_n, \tag{4.5}$$

where a is arbitrary. By substituting (4.1) into (4.5), c_k is given by

$$c_k = \sqrt{P_0}\left\{\frac{\sin(\pi k)}{(\pi k)}\left[\cos(B) - j\sin(B)\right] + j\frac{\sin(\pi k/2)}{(\pi k/2)}\sin(B)\right\}. \tag{4.6}$$

The modulation index B that is of interest is $\pi/2$. This corresponds to 180° phase shift between successive bit slots. By setting $B = \pi/2$ in (4.6), c_k is simplified to

$$c_k = j\sqrt{P_0}\left\{\frac{\sin(\pi k/2)}{(\pi k/2)} - \frac{\sin(\pi k)}{(\pi k)}\right\}. \tag{4.7}$$

It is clearly seen from (4.7) that when $k = 0$, $c_0 = 0$, and that $c_k = c_{-k}$ when $k \neq 0$. Moreover, $c_k = 0$ when k is an even integer. By using these observations, (4.4) reduces simply to

$$q_{nf}(\tau_n) = 2\sqrt{P_0}\sum_{k=1}^{+\infty} j\frac{\sin(\pi k/2)}{(\pi k/2)}\cos(\pi k\tau_n). \tag{4.8}$$

One obvious conclusion that can be drawn from (4.8) is that the square-wave phase modulation removes the DC component of the original signal, and generates sideband signals at normalized frequencies that are odd multiples of one-half. Thus, the first sideband ($k = 1$) will have a normalized frequency of one-half. This implies that $\left|q_{nf}(\tau_n)\right|$ is in fact a pulse train having a period of unity; however, if all sidebands are included, $\left|q_{nf}(\tau_n)\right|$ is just a signal having a constant magnitude of $\sqrt{P_0}$. In order to obtain a desired RZ pulse train, the unwanted sidebands have to be eliminated, which can be accomplished by employing a low-pass filter (a bandpass filter in practical implementation) with appropriate transfer function. The transfer function of a lowpass filter can be equivalently written as

$$H(f_n) = \left|H(f_n)\right| e^{j\xi(f_n)} \tag{4.9}$$

where $\left|H(f_n)\right|$ and $\xi(f_n)$ are the magnitude response and the phase response of the filter, respectively. The frequency parameter f_n in (4.9) is the physical baseband equivalent frequency normalized by the bit rate ($f_n = f/R_b$). Since $q_{nf}(\tau_n)$ given by (4.8) is periodic in time, its Fourier transform consists of only line spectra. Therefore, by using $H(f_n)$ given by (4.9) and $q_{nf}(\tau_n)$ given by (4.8), the signal at the filter output $q_{mod}(\tau_n)$ becomes

$$q_{mod}(\tau_n) = 2\sqrt{P_0}\sum_{k=1}^{+\infty} j\frac{\sin(\pi k/2)}{(\pi k/2)}\left|H\left(\frac{k}{2}\right)\right|\cos\left[\pi k\tau_n + \xi\left(\frac{k}{2}\right)\right]. \quad (4.10)$$

Since the magnitudes of $\frac{\sin(\pi k/2)}{(\pi k/2)}$ and $\left|H\left(\frac{k}{2}\right)\right|$ decreases as k increases, the terms associated with sufficiently large k in (4.10) can be neglected. Thus, the nonlinear phase response at high frequency can be neglected. That is, $\xi(k/2)$ in (4.10) can be safely approximated to be linear in frequency, and it only introduces a time delay T_d to the signal. By using this assumption, (4.10) can be written as

$$q_{mod}(\tau_n) = 2\sqrt{P_0}\sum_{k=1}^{+\infty} j\frac{\sin(\pi k/2)}{(\pi k/2)}\left|H\left(\frac{k}{2}\right)\right|\cos\left[\pi k(\tau_n - T_d)\right]. \quad (4.11)$$

If $q_{mod}(\tau_n)$ in (4.11) is to be an RZ pulse train, $q_{mod}(\tau_n)$ has to be equal to zero midway between the pulse peaks; i.e., at $\tau_n = k_1 + 1/2 + T_d$ where k_1 is an integer. By substituting $\tau_n = k_1 + 1/2 + T_d$ into (4.11), $q_{mod}(\tau_n)$ becomes

$$q_{mod}(\tau_n)\big|_{\tau_n = k_1 + 1/2 + T_d} = 2\sqrt{P_0}\sum_{k=1}^{+\infty} j\frac{\sin(\pi k/2)}{(\pi k/2)}\left|H\left(\frac{k}{2}\right)\right|\cos\left(\pi k k_1 + \frac{\pi k}{2}\right). \quad (4.12)$$

Since $\sin(\pi k/2)/(\pi k/2) \neq 0$ only when k is an odd integer, the odd values of k in (4.12) have to be considered. When k is odd, $\cos(\pi k k_1 + \pi k/2) = 0$. Consequently, $q_{mod}(\tau_n) = 0$ when $\tau_n = k_1 + 1/2 + T_d$. This proves that $q_{mod}(\tau_n)$ given by (4.10) is an RZ pulse train independent of the filter used. However, the shape of an individual pulse is mainly determined from the transfer function of the filter. For example, consider the filter to be an ideal rectangular filter (brick-wall filter) having a normalized cut-off bandwidth of unity (or equivalently one-half because the normalized frequencies of sidebands of $q_{nf}(\tau_n)$ are odd multiples of one-half). Then, $q_{mod}(\tau_n)$ in (4.11) becomes

$$q_{mod}(\tau_n) = \frac{4\sqrt{P_0}}{\pi}\cos(\pi\tau_n)e^{j\pi/2}. \quad (4.13)$$

The intensity $\left|q_{mod}(\tau_n)\right|^2$ is, therefore, given by

$$\left|q_{mod}(\tau_n)\right|^2 = \frac{P_0}{2}\left(\frac{4}{\pi}\right)^2\left[1+\cos(2\pi\tau_n)\right]. \quad (4.14)$$

It is clearly seen from (4.13) and (4.14) that $|q_{mod}(\tau_n)|$ is periodic with the period of unity, which is in fact a RZ pulse train. However, the phase of $q_{mod}(\tau_n)$ is still governed by (4.2). That is, the phase of $q_{mod}(\tau_n)$ given by (4.13) is reversed from pulse to pulse.

The previous example is rather ideal; however, RZ-pulse-train generation can still be accomplished with practical filters. For example, let the low-pass filter in Fig. 4.1 be a 2nd order Butterworth filter, whose transfer function is given by

$$H(f_n) = \frac{1}{\left(j\frac{f_n}{BW_{Tx,BB}}\right)^2 + \sqrt{2}\left(j\frac{f_n}{BW_{Tx,BB}}\right) + 1}, \tag{4.15}$$

where $BW_{Tx,BB}$ is the 3-dB baseband bandwidth of the filter normalized by the bit rate R_b. By substituting (4.15) into (4.10), the intensity $|q_{mod}(\tau_n)|^2$ and the phase $\phi(q_{mod}(\tau_n))$ of the signal at the filter output can be obtained. The signal at the data modulator input is plotted in Fig. 4.2a for the case of $BW_{Tx,BB} = 1.25$. It is clearly seen that from Fig. 4.2a that this technique can be used to generate the RZ pulse train. The asymmetry in an individual pulse is due to the nonlinear phase response of the filter. It should be noted that the phase of the pulse train shown in Fig. 4.2b is nearly identical to the square-wave phase function given by (4.2) with $B = \pi/2$. The filter slightly rounds off the corners of the phase function. That is, the filter affects the amplitude of the signal, but the phase characteristic is mostly preserved. From these results, square-wave phase modulating the CW signal and filtering is a potential technique to generate a RZ pulse train. A data modulator placed at the filter output is then used for modulating the generated RZ pulse train with the data pattern as shown in Fig. 4.1, and this signal format is called continuous-wave square-wave (CWSW).

4.1.1 Peak Intensity Enhancement (PIE)

Similar to the SWM signal format, the adjacent pulses in the CWSW signal have opposite signs. Thus, the growth of a spurious pulse due to the dispersion-induced overlap between adjacent pulses is suppressed, and the IFWM among pulses is minimized. However, the CWSW signal format has one additional advantage compared

with the SWM signal format. One may observe from Fig. 4.2a that an individual pulse in the RZ pulse train has very steep (sharp) edges on each side, which differs from a conventional pulse exhibiting smooth edges. Thus, the effect of dispersion on this pulse should be different from a smooth-edge pulse. In order to investigate this, we consider a single pulse that is gated "on" by the data modulator; i.e., the bit pattern is an isolated 1 ($\cdots 00100 \cdots$). It is then launched into a linear lossless optical fiber whose transfer function is given by [57]

$$H_o(f) = \exp\left[\frac{i}{2}\beta_2(2\pi f)^2 z\right], \tag{4.16}$$

which can be written in terms of normalized parameters as

$$H_o(f_n) = \exp\left[\frac{i}{2}\mathrm{sgn}(\beta_2)(a_0/T_b)^2(2\pi f_n)^2 z_n\right], \tag{4.17}$$

where z_n is the normalized transmission distance defined as the ratio between the physical distance z and the dispersion length L_D given by (3.29). Note that a_0 is related to the rms pulse width [see (3.29)] and is calculated from the numerically evaluated rms width of the pulse by using (3.20). The pulse shape at various normalized transmission distances z_n is plotted in Fig. 4.3a. The corresponding pulse peak and the rms width σ_q as a function of z_n are also shown in Fig. 4.3b. It is clearly seen from Fig. 4.3b that the peak intensity of $q_{out}(\tau_n)$ initially increases with an increase in z_n, and then decreases. This does not mean that the pulse is compressed because its rms width σ_q increases monotonically with z_n as shown in Fig. 4.3b.

Generally, the fiber dispersion smoothes a pulse, which in effect broadens the pulse, and decreases the pulse peak. Because of the very sharp edges of the pulse in this case, the effect of dispersion results in a broad pedestal (tail) on either side of the pulse, which can be easily seen in Fig. 4.3a when $z_n > 0$. The peak can even be higher than that at the fiber input when z_n is not too large. We call this phenomenon peak intensity enhancement (PIE). This is beneficial because a pulse is used for representing bit 1. The PIE in effect delays the reduction of the signal level for bit 1, therefore improving system performance, which will be discussed in the subsequent chapters. Note that the shape of

the pulse at the fiber input is controlled by the filter bandwidth. The larger the filter bandwidth, the sharper both edges of the pulse are. However, this also results in broader pedestals. The asymmetric shape of the pulse at the fiber input is due to the fact that the filter phase response is not linear, hence introducing waveform distortion. As the pulse propagates along the optical fiber, it adjusts itself to be more symmetric.

At this point, one may speculate that the PIE is mainly due to the pulse shape, which interacts with the dispersion differently from a conventional pulse shape. Unfortunately, an analytical model for the physical explanation of the PIE is difficult to develop from (4.10). In the following sections, we choose twin displaced Gaussian pulses as our mathematical model to analyze the PIE. The benefit of using the Gaussian pulses is that when an optical fiber is linear, the expression of the pulse shape at the fiber output can found in closed-form.

4.2 MATHEMATICAL MODEL

In this section, the mathematical model that is used for studying the PIE is provided. The considered pulse consists of two identical unchirped Gaussian pulses. The individual pulses have a normalized width of $a_n = a_0 / T_b$ and the peak amplitude of A_0. Both pulses are displaced from each other by δ in time. Note that all time-related parameters here are normalized by the bit period T_b unless otherwise specified. The mathematical expression of the input pulse $q(\tau_n)$ consisting of twin displaced Gaussian pulses is given by

$$q(\tau_n) = A_0 \left[\exp\left(-\frac{(\tau_n + \delta/2)^2}{2a_n^2} \right) + \exp\left(-\frac{(\tau_n - \delta/2)^2}{2a_n^2} \right) \right], \tag{4.18}$$

where τ_n is the normalized time. A sketch of the resultant pulse is shown on Fig. 4.4. The shape of the pulse given by (4.18) can be controlled by varying the normalized pulse width a_n of the individual pulses and the normalized pulse displacement δ. In this analysis, a linear lossless optical fiber having the length z is considered. The goal is to understand how the dispersion affects the pulse evolution. The reason for choosing the

two displaced Gaussian pulses is that this exhibits the essential features of PIE in a mathematically tractable model.

From (4.16), the transfer function of a linear lossless optical fiber can be written in terms of normalized parameters as

$$H_o(f_n) = \exp\left[\frac{i}{2}\mathrm{sgn}(\beta_2)a_n^2(2\pi f_n)^2 z_n\right], \tag{4.19}$$

where $z_n = z/L_D$ and L_D is the dispersion length of an individual Gaussian pulse involved in (4.18); i.e., $L_D = a_0^2/|\beta_2|$. By using (4.19), the mathematical expression of the pulse at the fiber output of the length z_n when the input pulse is given by (4.18) can be found from

$$q_{out}(\tau_n) = \int_{-\infty}^{\infty} Q(f_n)\exp\left[\frac{i}{2}\mathrm{sgn}(\beta_2)a_n^2(2\pi f_n)^2 z_n\right]\exp(-i2\pi f_n\tau_n)df_n, \tag{4.20}$$

where $Q(f_n)$ is the Fourier transform of the input pulse $q(\tau_n)$, and is given by

$$Q(f_n) = \int_{-\infty}^{\infty} q(\tau_n)\exp(i2\pi f_n\tau_n)d\tau_n. \tag{4.21}$$

By substituting (4.21) and (4.18) into (4.20), $q_{out}(\tau_n)$ is found to be given by

$$q_{out}(\tau_n) = \frac{A_0}{\left(1-i\,\mathrm{sgn}(\beta_2)z_n\right)^{1/2}}\left\{\exp\left[-\frac{(\tau_n+\delta/2)^2}{2a_n^2\left(1-i\,\mathrm{sgn}(\beta_2)z_n\right)}\right] + \exp\left[-\frac{(\tau_n-\delta/2)^2}{2a_n^2\left(1-i\,\mathrm{sgn}(\beta_2)z_n\right)}\right]\right\}. \tag{4.22}$$

From (4.22), the intensity of the output pulse $q_{out}(\tau_n)$ at the transmission distance of z_n is given by

$$|q_{out}(\tau_n)|^2 = \frac{A_0^2}{(1+z_n^2)^{1/2}}\left\{\exp\left[-\frac{(\tau_n+\delta/2)^2}{a_n^2(1+z_n^2)}\right] + \exp\left[-\frac{(\tau_n-\delta/2)^2}{a_n^2(1+z_n^2)}\right] + 2\cos\left[\frac{\tau_n\delta z_n}{a_n^2(1+z_n^2)}\right]\cdot\exp\left[-\frac{\tau_n^2+\delta^2/4}{a_n^2(1+z_n^2)}\right]\right\}. \tag{4.23}$$

These two equations, (4.22) and (4.23), are the key expressions that will be used throughout this analysis. When the input pulse given by (4.18) is considered, the sum of twin Gaussian pulses can result in either a single-peak pulse or a two-peak pulse

depending on the value of a_n and δ. For example, when a_n is fixed, at sufficiently large δ the resultant input pulse $q(\tau_n)$ will have two peaks.

In the case of a single-peak input pulse $q(\tau_n)$, the peak of the output pulse $q_{out}(\tau_n)$ is always at the center ($\tau_n = 0$) regardless of the normalized transmission distance z_n. In that case, the intensity of the peak as a function of z_n can be analytically determined from (4.23). On the other hand, when $q(\tau_n)$ has two peaks, $q_{out}(\tau_n)$ still has two peaks only during the initial propagation. However, when z_n is sufficiently large, $q_{out}(\tau_n)$ will have only a single peak at the center due to strong dispersion-induced overlap between the two input Gaussian pulses. Note that when $q_{out}(\tau_n)$ given by (4.22) has two peaks, the locations of pulse peaks, hence their intensity, as a function of z_n cannot be determined analytically from (4.23) without some simplification. By using (4.18) it is found that for $q(\tau_n)$ to have a single peak at the center, the ratio between the normalized pulse displacement δ and the normalized pulse width a_n has to be less than or equal to 2. The derivation of this condition is provided in Appendix A.

4.3 THRESHOLD FOR PIE

It is well known that as a chirp-free Gaussian pulse propagates along a linear lossless optical fiber, the pulse is broadened due to the effect of dispersion, and the pulse peak decreases correspondingly. Since $q(\tau_n)$ given by (4.18) is a Gaussian pulse when the pulse displacement δ is zero, there should exist a threshold value of δ relative to the pulse width a_n for which the PIE can occur. The existence of the threshold can be intuitively understood from the fact that the PIE does not occur on all pulse shapes. The larger the pulse displacement δ, the more is the dissimilarity between the shape of $q(\tau_n)$ and that of the Gaussian pulse.

First we assume that PIE can occur when the input pulse $q(\tau_n)$ has a single peak. In this case the peak of the output pulse $q_{out}(\tau_n)$ is always at the center ($\tau_n = 0$). By setting $\tau_n = 0$ in (4.18), the pulse peak at the fiber input is given by

$$|q(0)|^2 = 4A_0^2 \exp\left(-\frac{\phi^2}{4}\right), \tag{4.24}$$

where $\phi = \delta / a_n$, which indicates how much the input twin Gaussian pulses are spaced apart relative to the pulse width of the individual pulses. If the peak input power is P_0, then A_0 has to be equal to

$$A_0 = \frac{\sqrt{P_0}}{2} \exp\left(\frac{\phi^2}{8}\right). \tag{4.25}$$

By substituting A_0 given by (4.25) into (4.23), and setting $\tau_n = 0$, the intensity at the center of $q_{out}(\tau_n)$ is given by

$$|q_{out}(0)|^2 = \frac{P_0}{(1+z_n^2)^{1/2}} \exp\left[\frac{\phi^2 z_n^2}{4(1+z_n^2)}\right]. \tag{4.26}$$

When (4.26) is inspected, the peak power of $q_{out}(\tau_n)$ can be greater than the input peak power P_0 when the exponential term, which is also a function of ϕ, is larger than the denominator for a given z_n. This implies that the PIE can occur when ϕ is larger than a certain value, confirming that there exists the threshold of ϕ for the PIE to occur.

When the PIE takes place, $\partial|q_{out}(0)|^2 / \partial z_n \geq 0$ up to a certain z_n. Moreover, z_n that satisfies $\partial|q_{out}(0)|^2 / \partial z_n = 0$ is the distance at which the PIE is strongest (the peak is highest) for a given ϕ. By taking the derivative of $|q_{out}(0)|^2$ with respect to z_n, and setting the resultant expression to zero, the optimum transmission distance $z_{n,Opt}$ at which the peak is highest for a given ϕ is given by

$$z_{n,Opt} = \left(\frac{\phi^2}{2} - 1\right)^{1/2}. \tag{4.27}$$

The minimum $z_{n,Opt}$ in (4.27) corresponds to the threshold value of ϕ for which the PIE can occur. Since the minimum value of $z_{n,Opt}$ is zero, the threshold value of ϕ is equal to $\sqrt{2}$ ($\phi_{th} = \sqrt{2}$). By substituting z_n in (4.26) by $z_{n,Opt}$ given by (4.27), the peak power of the pulse at $z_{n,Opt}$ is given by

$$\left|q_{out,max}(0)\right|^2 = \frac{P_0}{(1+z_{n,Opt}^2)^{1/2}} \exp\left(\frac{z_{n,Opt}^2}{2}\right), \tag{4.28a}$$

or

$$\left|q_{out,max}(0)\right|^2 = \frac{\sqrt{2}P_0}{\phi} \exp\left(\frac{\phi^2 - 2}{4}\right). \tag{4.28b}$$

As seen from (4.28a), the pulse peak power at $z_{n,Opt}$ increases with the increase in $z_{n,Opt}$. However, it should be noted that (4.28a) and (4.28b) are derived under the assumption that $q_{out}(\tau_n)$ has only one peak; thus, they are valid for $\sqrt{2} \le \phi \le 2$, which corresponds to $0 \le z_{n,Opt} \le 1$.

Shown in Fig. 4.5 are the plots of the pulse peak power $\left|q_{out}(0)\right|^2$ given by (16) as a function of normalized transmission distance z_n at different values of ϕ when the input peak power $P_0 = 1$. It is clearly seen from Fig. 4.5 that at small ϕ ($\phi < \sqrt{2}$), the peak of the pulse decreases with the increase in z_n as expected. When ϕ is larger than $\sqrt{2}$, the PIE starts be observable. For $\phi = 2$, the pulse peak is highest at $z_n = 1.0$, which is $z_{n,Opt}$ that can be calculated by using (4.27). It should be noted that the PIE increases with ϕ for the case of a single-peak pulse. For a given a_n, as $\phi = \delta / a_n$ increases, the steepness (sharpness) of the input-pulse edges relative to the pulse width (the ratio between the rise time (or fall time) and the pulse width) is increased as seen from the right insets of Fig. 4.5. This confirms our postulation that for a pulse to exhibit the PIE, its edges have to be sufficiently steep (sharp). However, the physical interaction between such a pulse and the dispersion still needs to be investigated. Since the output pulse $q_{out}(\tau_n)$ is complex [see (4.22)], the appropriate way to understand the PIE is to observe the intensity and the phase-related parameters of the pulse as it propagates along an optical fiber. This is provided in the next section.

4.4 PIE EXPLANATION IN THE TIME DOMAIN

In general, the effect of dispersion on a conventional pulse (a single Gaussian pulse, for example) is to cause the different parts of the pulse to travel at different speeds,

which leads to pulse broadening. For example, let δ in (4.18) be zero and $A_0 = \sqrt{P_0}/2$ so that the input pulse $q(\tau_n)$ is a Gaussian pulse having pulse width a_n and peak input power P_0. By using (4.22) the output pulse $q_{out}(\tau_n)$ at the normalized transmission distance z_n is given by [57]

$$q_{out}(\tau_n) = \frac{\sqrt{P_0}}{\left(1 - i\,\mathrm{sgn}(\beta_2) z_n\right)^{1/2}} \exp\left[-\frac{\tau_n^2}{2a_n^2 \left(1 - i\,\mathrm{sgn}(\beta_2) z\right)_n} \right]. \tag{4.29}$$

It should be noted that $q_{out}(\tau_n)$ can be written as

$$q_{out}(\tau_n) = \left| q_{out}(\tau_n) \right| \exp\left[i\zeta(\tau_n) \right] \tag{4.30}$$

where $\zeta(\tau_n)$ is the phase of $q_{out}(\tau_n)$ and is given by [57]

$$\zeta(\tau_n) = -\frac{\mathrm{sgn}(\beta_2) z_n}{2\left(1 + z_n^2\right)} \frac{\tau_n^2}{a_n^2} + \frac{\mathrm{sgn}(\beta_2)}{2} \tan^{-1}(z_n). \tag{4.31}$$

From (4.31) it can be seen that the effect of dispersion is to induce a quadratic phase variation across the pulse for a given z_n. Since the phase variation $\zeta(\tau_n)$ is not constant with time τ_n, the dispersion in fact causes an instantaneous frequency shift across the pulse. By using (4.31), the normalized instantaneous frequency $\delta\omega_n(\tau_n)$ is given by

$$\delta\omega_n(\tau_n) = -\frac{\partial \zeta(\tau_n)}{\partial \tau_n} = \frac{\mathrm{sgn}(\beta_2) z_n}{\left(1 + z_n^2\right)} \frac{\tau_n}{a_n^2}. \tag{4.32}$$

Generally, the instantaneous frequency variation $\delta\omega_n(\tau_n)$ is called frequency chirp. As seen from (4.32) the fiber dispersion results in a uniform frequency chirp across the pulse. Note that the instantaneous frequency $\delta\omega_n(\tau_n)$ is also a function of $\mathrm{sgn}(\beta_2)$. In the normal dispersion regime ($\mathrm{sgn}(\beta_2) = +1$), the leading edge of the pulse ($\tau_n < 0$) is red shifted ($\delta\omega_n$ is negative) while the trailing edge of the pulse is blue shifted ($\delta\omega_n$ is positive), whereas the reverse is true in the anomalous dispersion regime. A blue component travels slower than a red component in the normal dispersion regime, and faster in the anomalous dispersion regime. Consequently, independent of the sign of the dispersion, the leading edge of the pulse propagates along an optical fiber at the speed higher than the trailing edge, which results in the pulse broadening. However, different

pulses have different spectral content; hence, the way the dispersion interacts with those pulses is dependent on the pulse shape.

4.4.1 Single-Peak Pulse

Shown in Fig. 4.6a is the evolution of $|q_{out}(\tau_n)|^2$ calculated from (4.23) when $\phi = 2.0$, $P_0 = 1$, $a_0 = 0.15$ and $\text{sgn}(\beta_2) = +1$ (normal dispersion regime). The corresponding instantaneous frequency shift $\delta\omega_n(\tau_n)$ of $q_{out}(\tau_n)$ numerically evaluated from (4.22) is also plotted in Fig. 4.6b. When $|q_{out}(\tau_n)|^2$ is considered, its peak at the center initially increases, and is highest when $z_n = 1.0$. When $z_n > 1.0$, the peak starts to decrease. Note that the pulse is broadened monotonically by the dispersion, which can be observed from the increase in the tails of the pulse (see Fig. 4.6a at τ_n around ± 0.5). When the instantaneous frequency shift $\delta\omega_n(\tau_n)$ of $q_{out}(\tau_n)$ is considered, unlike a conventional pulse (a single Gaussian pulse for example), the leading edge of the pulse is not uniformly red shifted ($\delta\omega_n < 0$), and the trailing edge of the pulse is not uniformly blue shifted ($\delta\omega_n > 0$) when $z_n < 1.0$ (note that $z_{n,Opt} = 1.0$ in this case). The signal component on the leading edge near the center is blue shifted, while the signal component on the trailing edge near the center is red shifted. Note that the sign of instantaneous-frequency shift is opposite to the case currently discussed when $\text{sgn}(\beta_2) = -1$. Since the blue components travel slower than the red components in the normal dispersion regime ($\text{sgn}(\beta_2) = +1$), the blue-shifted (red-shifted) pulse components on the leading edge (the trailing edge) near the center are retarded (advanced). That is, the dispersion causes the signal components around the center of the pulse to move toward the center; hence increasing the pulse peak. However, when the signal components around the tails of the pulse are considered, they are chirped by the dispersion normally. Thus, the signal components around the tails are stretched away from the center of the pulse as usual, which results in the pulse broadening.

When $z_n > 1.0$, the peak starts to decreases (see Fig. 4.5 for the plot corresponding to $\phi = 2.0$), and the leading edge (trailing edge) near the center of the

pulse is no longer blue shifted (red shifted). This can be seen from Fig. 4.6b on the plot corresponding to $z_n = 2$. Note that at the optimum transmission distance $z_{n,Opt}$ where the peak is highest, the pulse starts to be chirped by the dispersion the same way as a conventional pulse. Therefore, when $z_n > z_{n,Opt}$, the signal components on the leading edge of the pulse travel faster than those on the trailing edge, which causes the pulse peak at the center to decrease similar to a conventional pulse.

The mathematical reason behind the sum of two Gaussian pulses $q_{out}(\tau_n)$ not being chirped monotonically by the dispersion can be explained as follows. In general, the dispersion uniformly chirps a Gaussian pulse. Since the considered optical fiber is linear, superposition can be applied. The electric field of the resultant pulse $q_{out}(\tau_n)$ at transmission distance z_n is the sum of the electric fields of two Gaussian pulses, which are identically chirped by the dispersion. However, the phase of the resultant pulse is not simply the sum of the phases of those two Gaussian pulses. The interference between those two Gaussian pulses results in the instantaneous frequency shift $\delta\omega_n(\tau_n)$ of the resultant pulse $q_{out}(\tau_n)$ not being monotonic in time when ϕ is larger than $\sqrt{2}$, which leads to the PIE up to a certain distance $z_{n,Opt}$. One conclusion that can be drawn from the observation of the instantaneous frequency $\delta\omega_n(\tau_n)$ is that for a pulse to undergo the PIE, its shape has to be optimally designed so that its interaction with the dispersion does not result in the pulse being uniformly chirped. By continuity the increase in the PIE with ϕ suggests that the PIE can still occur in the case of a two-peak pulse.

4.4.2 Two-Peak Pulse

For the input pulse $q(\tau_n)$ given by (4.18) to have two peaks, $\phi = \delta / a_n$ has to be larger than 2. In this case, as $q(\tau_n)$ initially propagates along an optical fiber, the intensity profile still has two peaks. As the transmission distance increases, those two initial peaks start to vanish, and at sufficiently large transmission distance the output pulse $q_{out}(\tau)$ will have only a single peak at the center. This situation differs from the case when the input pulse $q(\tau_n)$ has only a single peak. Plotted in Fig. 4.7 is the pulse

peak regardless of its position as a function of normalized transmission distance z_n when $\phi > 2$. Note that the case of $\phi = 2$ (solid line) is for comparison. The insets on the right are the intensity profiles of the input pulse $|q(\tau_n)|^2$ corresponding to the curves in the main figure. It is seen from Fig. 4.7 that when $\phi > 2$, the pulse peak decreases with z_n at the beginning of the propagation. However, after a certain z_n, the peak starts to increase again, and at large z_n, the peak decreases with z_n. This behavior can be explained as follows.

The dispersion causes two displaced Gaussian pulses in $q(\tau_n)$ to spread in time; hence, their peaks decrease. Since the peaks of $q(\tau_n)$ originate from the peaks of those two Gaussian pulses when they are sufficiently separated, the peaks of the output pulse $q_{out}(\tau_n)$ decreases during the initial propagation. At the same time, the intensity around the center of $q_{out}(\tau_n)$ starts to increase. Due to the nonuniformity of the instantaneous-frequency shift $\delta\omega_n(\tau_n)$ around the center of $q_{out}(\tau_n)$, the signal component on the leading edge around the center of $q_{out}(\tau_n)$ is retarded, while the signal component on the trailing edge around the center of $q_{out}(\tau_n)$ is advanced, similar to the case when $q(\tau_n)$ has one peak. The peak at the center of $q_{out}(\tau_n)$ starts to increase, while those initial peaks away from the center keep reducing as z_n increases. After a certain z_n, the peak at the center dominates those two initial peaks, which begin to vanish with the increase in z_n. Therefore, the peak of $q_{out}(\tau_n)$ increases again. For example, when $z_n > 0.8$, the peak of $q_{out}(\tau_n)$ starts to increase again in the case of $\phi = 3.0$ as shown in Fig. 4.7. The illustration of pulse evolution ($|q_{out}(\tau_n)|^2$ as a function of z_n) when $\phi = 3.0$ is shown in Fig. 4.8, which corresponds to the dashed curve in Fig. 4.7. It is seen that at $z_n = 1.0$, $q_{out}(\tau_n)$ has only a single peak, although the input pulse has two peaks. The peak of the pulse reaches its highest point at $z_{n,Opt}$, which is approximately equal to 1.8 in this case. It is clearly seen that the peak of $q_{out}(\tau_n)$ at $z_{n,Opt}$ is greater than the input peak. This shows that the PIE can still occur even when the input pulse $q(\tau_n)$ has two peaks. When

$z_n > z_{n,Opt}$, the peak of $q_{out}(\tau_n)$ starts to decrease. This is because the interaction between the dispersion and $q_{out}(\tau_n)$ no longer causes the nonuniform instantaneous-frequency shift $\delta\omega_n(\tau_n)$ around the center of $q_{out}(\tau_n)$. Hence, the peak of $q_{out}(\tau_n)$ decreases with the increase in z_n, which resembles the behavior of a conventional pulse under the presence of dispersion as shown in Fig. 4.8.

4.5 Upper Bound on Pulse Separation

Recall that $\phi = \delta / a_n$ is the ratio between the displacement of the two input Gaussian pulses and the pulse width of the individual pulses. As ϕ increases, those two pulses are separated father apart relative to their pulse width. Hence, larger dispersion (longer z_n) is required to form the peak at the center of $q_{out}(\tau_n)$, as ϕ increases, which can be seen in Fig. 4.7. The distance z_n at which the peak starts to increase again increases with ϕ when $\phi > 2$. In addition, one can notice from Fig. 4.7 that when ϕ is larger than a certain value ($\phi = 4$, for example), the peak of the output pulse $q_{out}(\tau_n)$ cannot be greater than the peak at the input. This suggests that there exists an upper bound on ϕ for which PIE can occur. Note that the upper bound on ϕ also implies that there is a maximum on the optimum transmission distance $z_{n,Opt}$.

The existence of that upper bound is the result of the fact that the initial overlap between two Gaussian pulses at the input decreases with ϕ as shown in the right insets of Fig. 4.7. When two input Gaussian pulses are overly separated, large dispersion (long z_n) is necessary for the peak at the center of $q_{out}(\tau_n)$ to be able to form from the overlap between those two pulses. Large transmission distance implies that those two initial pulses broaden severely. This causes the output pulse $q_{out}(\tau_n)$ to have a long tail on each side, and from energy conservation the energy at the center is small. Thus, when ϕ is too large, the peak at the center of $q_{out}(\tau_n)$ cannot be greater than the peaks of $q(\tau_n)$.

When $q(\tau_n)$ has two peaks, (4.25) cannot be used to set the input peak power to P_0 because (4.25) is derived under the condition that $q(\tau_n)$ has only a single peak at the

center ($\tau_n = 0$). In order to set the input peak power to P_0 when $\phi > 2$, the locations of the peaks have to be determined first. In fact, the locations of the peaks are not at $\pm\delta/2$ (see Fig. 4.4) because the tail of one input pulse overlaps with the center of another pulse, hence shifting the peaks of $q(\tau_n)$ away from $\pm\delta/2$. Unfortunately, the peak locations cannot be determined analytically. However, the peak locations are near the vicinity of $\pm\delta/2$; thus, it is appropriate to approximate the peak locations to be at $\pm\delta/2$. Note that as δ increases, the overlap decreases; hence, the exact locations of the peaks become closer to $\pm\delta/2$. By using this approximation, for the input peak power of P_0, the peak amplitude of individual Gaussian pulses A_0 in (4.18) has to be equal to

$$A_0 = \frac{\sqrt{P_0}}{\left[1+\exp\left(-\frac{\phi^2}{2}\right)\right]}. \tag{4.33}$$

When the pulse $q_{out}(\tau_n)$ undergoes the PIE, the peak of $q_{out}(\tau_n)$ is at the center. By substituting (4.33) into (4.23), the peak of $q_{out}(\tau_n)$ is governed by

$$\left|q_{out}(0)\right|^2 = \frac{4P_0}{(1+e^{-\phi^2/2})^2(1+z_n^2)^{1/2}}\exp\left[-\frac{\phi^2}{4(1+z_n^2)}\right]. \tag{4.34}$$

Since $q_{out}(\tau_n)$ has one peak when the PIE is strongest, the optimum transmission distance $z_{n,Opt}$ at which the peak is highest for a given ϕ derived earlier is still valid. By substituting z_n in (4.34) by $z_{n,Opt}$ given by (4.27), the peak of $q_{out}(\tau_n)$ when the PIE is strongest is given by

$$\left|q_{out}(z_{n,Opt},0)\right|^2 = \frac{(4\sqrt{2}e^{-1/2})P_0}{\left[1+e^{-\phi^2/2}\right]^2\phi}, \tag{4.35a}$$

which can also be written as a function of $z_{n,Opt}$ as

$$\left|q_{out}(z_{n,Opt},0)\right|^2 = \frac{(4e^{-1/2})P_0}{\left[1+e^{-(1+z_{n,Opt})}\right]^2(1+z_{n,Opt}^2)^{1/2}}. \tag{4.35b}$$

By setting $\left|q_{out}(z_{n,Opt},0)\right|^2$ in (4.35a) to P_0, the upper bound of ϕ is found to be equal to 3.41. At this value of ϕ, the peak power of the output pulse $q_{out}(\tau_n)$ is equal to the input

peak power at $z_{n,Opt}$, which is equal to 2.19. Note that this value of $z_{n,Opt}$ is also the maximum normalized transmission distance, at which the PIE can occur.

The plot of $z_{n,Opt}$ as a function of ϕ is provided in Fig. 4.9. It should be noted that (4.27) yields the exact normalized transmission distance at which the PIE is strongest. This is because when the PIE is strongest, the output pulse $q_{out}(\tau_n)$ has only one peak at the center ($\tau_n = 0$). As two input Gaussian pulses are separated farther apart, a stronger effect of the dispersion is required so that the overlap between those two pulses is sufficient to induce the PIE. Therefore, $z_{n,Opt}$ increases with ϕ, which represents the pulse displacement. Shown in Fig. 4.10 is the peak power of the output pulse $q_{out}(\tau_n)$ at $z_{n,Opt}$ when the peak input power P_0 is equal to unity. The solid curve is calculated by using (4.28b) which is valid for $\phi \le 2$ whereas the dashed curve corresponds to (4.35a), which is derived for $\phi > 2$. The actual value of $|q_{out}(0)|^2$ at $z_{n,Opt}$ calculated from (4.23) when the input peak power is set to P_0 by numerically adjusting A_0 is also shown in Fig. 4.10 (dashed-dot curve) for comparison. For $\phi \le 2$, all analytical expressions are derived without any approximations; therefore, the curve evaluated from (4.28b) coincides with the actual results. However, when $\phi > 2$, $|q_{out}(0)|^2$ evaluated from (4.28b) starts to deviate from the actual result, and the disagreement between those two increases with ϕ. This is because (4.28b) is derived under the assumption that the input pulse $q(\tau_n)$ has only a single peak, which corresponds to $\phi \le 2$. On the other hand, $|q_{out}(0)|^2$ at $z_{n,Opt}$ calculated from (4.35a), which is derived for $\phi > 2$, becomes more accurate as ϕ increases. This is due to the fact that the locations of the input peaks become closer to $\pm\delta/2$ as ϕ increases.

It is seen from Fig. 4.10 that the actual value of $|q_{out}(0)|^2$ at $z_{n,Opt}$ increases initially with ϕ. However, at large ϕ, $|q_{out}(0)|^2$ decreases with the increase in ϕ. When ϕ is larger than its threshold value ($\sqrt{2}$), the PIE starts to take place. As ϕ increases, the nonuniform instantaneous-frequency shift $\delta\omega_n(\tau_n)$ around the center of $q_{out}(\tau_n)$ caused

by the dispersion is stronger. Therefore, $|q_{out}(0)|^2$ at $z_{n,Opt}$ increases with ϕ initially. However, the overlap between two input Gaussian pulses (the signal component around the center of the input pulse $q(\tau_n)$) decreases with ϕ. Therefore, when ϕ is larger than a certain value, which is numerically found to be equal to 2.3, $|q_{out}(0)|^2$ at $z_{n,Opt}$ decreases with ϕ due to less initial overlap between two input Gaussian pulses.

4.6 OPTIMUM RATIO BETWEEN PULSE DISPLACEMENT AND PULSE WIDTH

The PIE is the phenomenon by which the interaction between the dispersion and the pulse can result in an increase in the pulse peak power during initial propagation. This phenomenon in effect delays the reduction of the pulse peak at large transmission distance z_n. For a given ϕ (pulse shape), there exists an optimum transmission distance $z_{n,Opt}$ at which the PIE is strongest (the peak power of the output pulse is highest). This has already been discussed in the previous sections. However, for a given normalized transmission distance z_n, there is also the optimum value of ϕ (ϕ_{Opt}) that maximizes the peak power of the output pulse $q_{out}(\tau_n)$.

For a given z_n, ϕ_{Opt} has to satisfy $\partial|q_{out}(0)|^2/\partial\phi = 0$. By using (4.34), it is found that ϕ_{Opt} is simply given by

$$\phi_{Opt} = \left[2\ln(3+4z_n^2)\right]^{1/2}. \tag{4.36}$$

At $\phi = \phi_{Opt}$, $|q_{out}(0)|^2$ given by (4.34) becomes

$$|q_{out}(0)|^2 = \frac{P_0(3+4z_n^2)^2}{4(1+z_n^2)^{3/2}}\exp\left[-\frac{\ln(3+4z_n^2)}{2(1+z_n^2)}\right]. \tag{4.37}$$

It should be noted that ϕ_{Opt}, given by (4.36), and the corresponding $|q_{out}(0)|^2$, given by (4.37), are derived under the approximation that the peaks of the pulse at the fiber input are at $\pm\delta/2$ which is for $\phi > 2$. Thus, (4.36) and (4.37) should become accurate at large ϕ_{Opt}. In order to verify the accuracy of (4.36) and (4.37), ϕ_{Opt} and $|q_{out}(0)|^2$ as a function

of z_n are compared with the actual results as shown in Fig. 4.11 and Fig. 4.12, respectively, when the peak input power $P_0 = 1$. As seen from Fig. 4.11, ϕ_{Opt} increases with z_n; therefore, (4.36) is more accurate at large z_n. Accordingly, the accuracy of (4.37) for the prediction $|q_{out}(0)|^2$ at ϕ_{Opt} increases with z_n as shown in Fig. 4.12.

The increase of ϕ_{Opt} with z_n comes from the fact that as ϕ increases, the initial overlap between the two input Gaussian pulses decreases; hence, larger dispersion (longer z_n) is necessary for forming the peak at the center of $q_{out}(\tau_n)$. At ϕ_{Opt}, the peak power of the output pulse $q_{out}(\tau_n)$ can be greater than that of the input pulse when z_n is not too large. As seen from Fig. 4.12, the PIE is effective up to several dispersion lengths. The peak of $q_{out}(\tau_n)$ can be maintained to be larger than the input peak power up to approximately $z_n = 3$. The result shown in Fig. 4.12 suggests that by choosing ϕ properly, the interaction between the dispersion and the pulse shape can be exploited to delay the reduction of the peak of the output pulse. This is beneficial in a communication system where a pulse is generally used for representing bit 1. In practice, delaying the reduction of the pulse peak allows longer transmission distance for a given input peak power or lower transmitted power for a given transmission distance.

4.7 FREQUENCY CHARACTERISTIC

In the case of a single Gaussian pulse, its Fourier transform is still Gaussian. However, for the sum of two displaced Gaussian pulses, the Fourier transform is no longer Gaussian. When an optical fiber is linear, its transfer function can be modeled as an all-pass filter with nonlinear phase response as expressed in (4.19). In the frequency domain a dispersive linear optical fiber affects only the phase of the Fourier transform of the signal. Hence, the PSD of the signal at any normalized transmission distance z_n is identical to that at the fiber input. By substituting $q(\tau_n)$ given by (4.18) into (4.21), the Fourier transform of $q(\tau_n)$ is given by

$$Q(f_n) = (2\pi)^{1/2} 2A_0 T_b a_n \cos(\pi \delta f_n) \exp\left(-2\pi^2 a_n^2 f_n^2\right). \tag{4.38}$$

It is clearly seen from (4.38) that when two Gaussian pulses are added together, the corresponding Fourier transform is the product of the Fourier transform of an individual Gaussian pulse (the exponential term) and the cosine term. The cosine term is the result of those two Gaussian pulses not being colocated. Since the coefficients in (4.38) only affect the amplitude of $Q(f_n)$, not its shape, they can be ignored by normalizing $Q(f_n)$ so that its peak at $f_n = 0$ has unit amplitude for ease of comparison. The normalized version of $Q(f_n)$ is simply given by

$$Q_n(f_n) = \cos(\pi\delta f_n)\exp\left(-2\pi^2 a_n^2 f_n^2\right). \tag{4.39}$$

When (4.39) is considered, the period of the cosine term is inversely proportional to δ. For a fixed normalized pulse width a_n, as the pulse displacement δ increases, the sidelobes of $Q_n(f_n)$ increase relative to the main lobe. This is shown in Fig. 4.13 where $Q_n(f_n)$ is plotted for different values of δ when a_n is fixed to 0.15.

It is clearly seen from Fig. 4.13 that as δ increases (ϕ increases), the level of the first negative sidelobes increases. This suggests that the negative sidelobes are the key that leads to the occurrence of PIE. This is because the sign of negative sidelobes are opposite to the mainlobe. Hence, the negative sidelobes will interact with the dispersion differently from the mainlobe. Although the energy contained in the negative sidelobes is less than that in the mainlobe, the negative sidelobes experience stronger nonlinear phase shift since the level of nonlinear phase shift is quadratic in frequency, which can be seen from (4.19). To achieve the PIE, the energy contained in the negative sidelobes has to be sufficient in order that the interaction between the negative sidelobes and the dispersion overcomes the interaction between the mainlobe and the dispersion. Hence, there exists the threshold in δ for a given a_n, which in fact imposes the threshold in ϕ. As ϕ (δ) increases, the effect of the negative sidelobes on the pulse propagation is stronger. Thus, the PIE initially increases with ϕ (δ), which is consistent with the result shown in Fig. 4.10. It should be noted that as ϕ increases, the first positive sidelobes also increases. This can be seen from Fig. 4.13 when $\delta = 0.6$ ($\phi = 4.0$). The interaction between the positive sidelobes and the dispersion is similar to the interaction between the mainlobe and the dispersion due to the fact that both the positive sidelobes and the mainlobe have

the same sign. Therefore, when ϕ (or δ) larger than a certain value, the effect of the negative sidelobes on pulse propagation starts to be less effective because the combined effects of the mainlobe and the positive sidelobes start to increase. This causes the reduction of the PIE when ϕ is larger than a certain value, which in fact results in the existence of the upper bound of ϕ for which the PIE can occur.

Although the width of the mainlobe of $Q_n(f_n)$ decreases with the increase in ϕ for a given a_n, the level of the sidelobes increases with ϕ. This observation suggests that there is the value of ϕ at which the rms width of $Q_n(f_n)$ is minimum. The benefit of having narrow spectral width is that the available transmission bandwidth can be utilized more effectively. By using (4.39), the rms spectral width of $q(\tau_n)$ is given by

$$\sigma_{f_n} = \left[\frac{1 + e^{-\phi^2/4}\left(1 - \dfrac{\phi^2}{4}\right)}{2a_n^2(2\pi)^2\left(1 + e^{-\phi^2/4}\right)} \right]^{1/2} . \tag{4.40}$$

By differentiating σ_{f_n} given by (4.40) with respect to ϕ and setting the resultant expression to zero, the value of ϕ that satisfies that equality is the one that minimize the rms spectral width of $q(\tau_n)$. By doing so, it is found that the rms spectral width of $q(\tau_n)$ is minimum when $\phi = 2.26$. Despite having minimum rms spectral width, the input pulse $q(\tau_n)$ with $\phi = 2.26$ also exhibits PIE because this value of ϕ is larger than the PIE threshold ($\sqrt{2}$). Thus, the benefit of PIE is achieved as well as effective spectral utilization.

4.8 SUMMARY

In this chapter, a new method for generating an alternate-sign RZ pulse train suitable for carrying data in a dispersive medium, such as an optical fiber, is discussed. The signal format that uses this RZ pulse train is termed continuous-wave square-wave (CWSW). The major advantage of this signal format comes from the shape of individual pulses in the RZ pulse train. Unlike a conventional pulse whose peak decreases

monotonically as that pulse propagates along an optical fiber, the peak of the RZ pulse generated from our proposed technique increases during the initial propagation. We called this phenomenon peak intensity enhancement (PIE). The PIE in effect delays the reduction of the pulse peak, which is beneficial because the pulse peak in practice represents the signal level for bit 1. In the theoretical analysis of the PIE, the CWSW pulse is modeled as the sum of two displaced Gaussian pulses. Although the actual CWSW pulse differs considerably from this, the two displaced Gaussian pulse model illustrates the essential features of PIE in an analytically tractable model that provides an in-depth understanding of the PIE. Due to its simple system implementation while providing an additional advantage via the PIE, the CWSW signal format is promising. However, its performance compared with other modulation formats still requires investigation. The performance comparisons between the CWSW signal format and other signal formats are the main subjects of the remaining chapters in this dissertation.

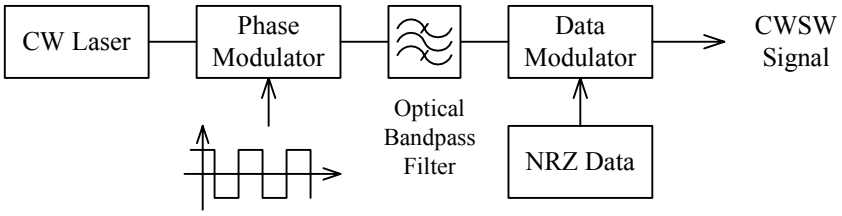

Fig. 4.1: Schematic diagram of the transmitter for CWSW signal.

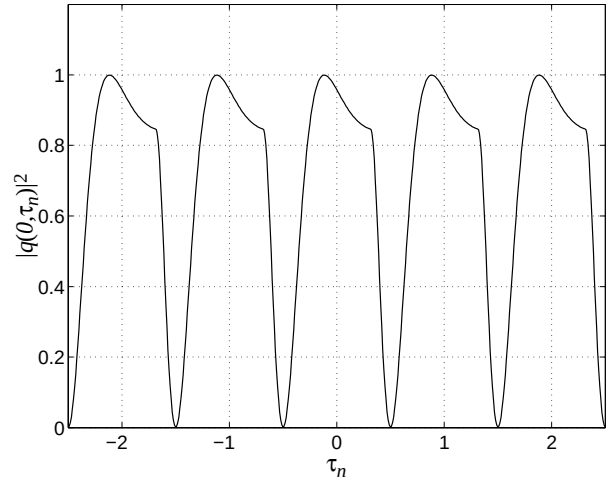

(a)

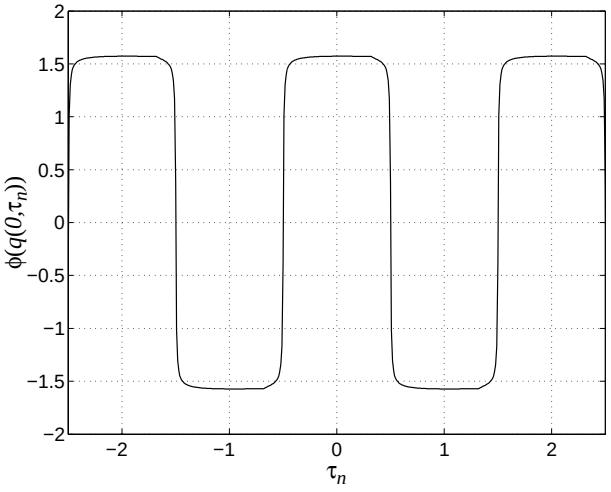

(b)

Fig. 4.2: Alternate-sign RZ pulse train generated from CWSW technique when $BW_{Tx,BB} = 1.25$. (a) Intensity of RZ pulse train. (b) Corresponding phase variation as a function of normalized time.

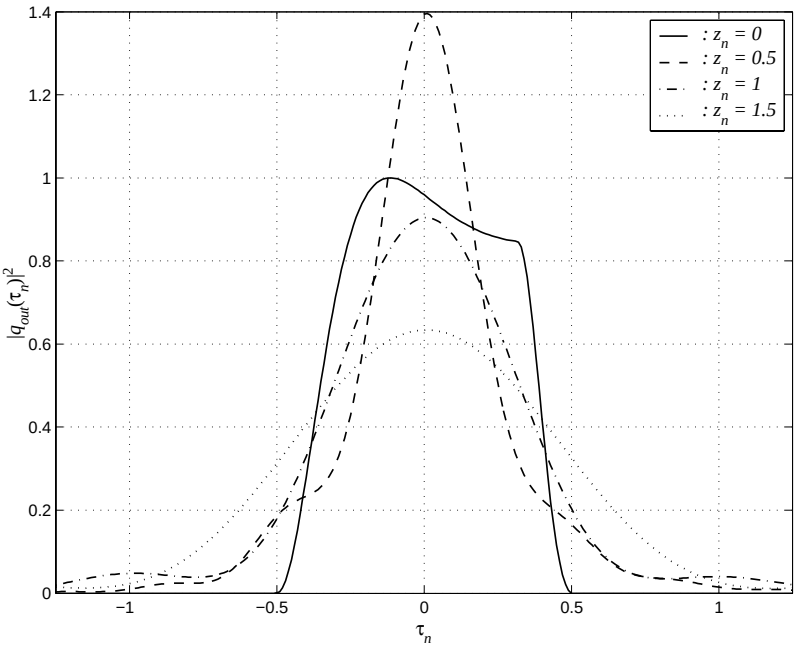

(a)

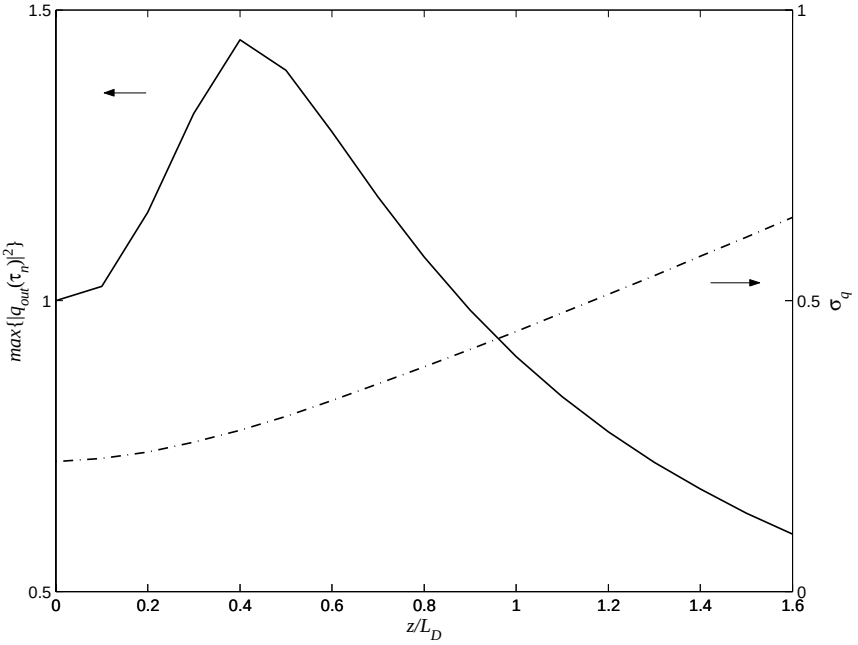

(b)

Fig. 4.3: (a) Snapshots of pulse evolution at different $z_n = z / L_D$ of a single pulse gated from RZ pulse train generated from CWSW technique when $BW_{Tx,BB} = 1.25$. (b) Corresponding pulse peak and RMS width as a function of z_n. (L_D is the dispersion length.)

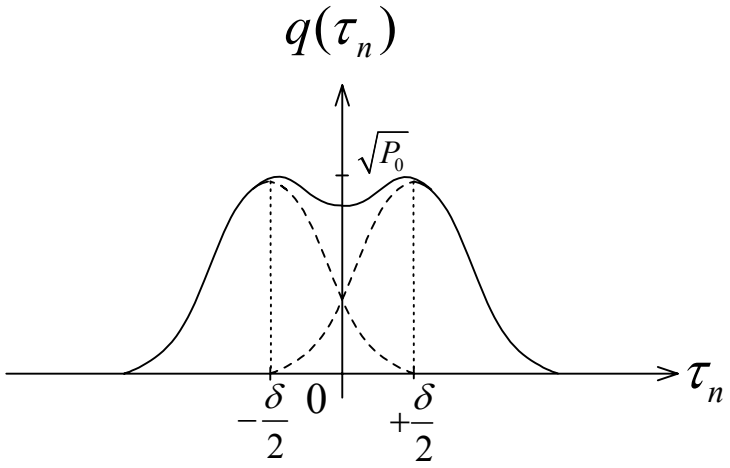

Fig. 4.4: Illustration of twin displaced Gaussian pulses. The solid curve corresponds to the sum of two Gaussian pulses. The dash curves represent the shape of individual Gaussian pulses.

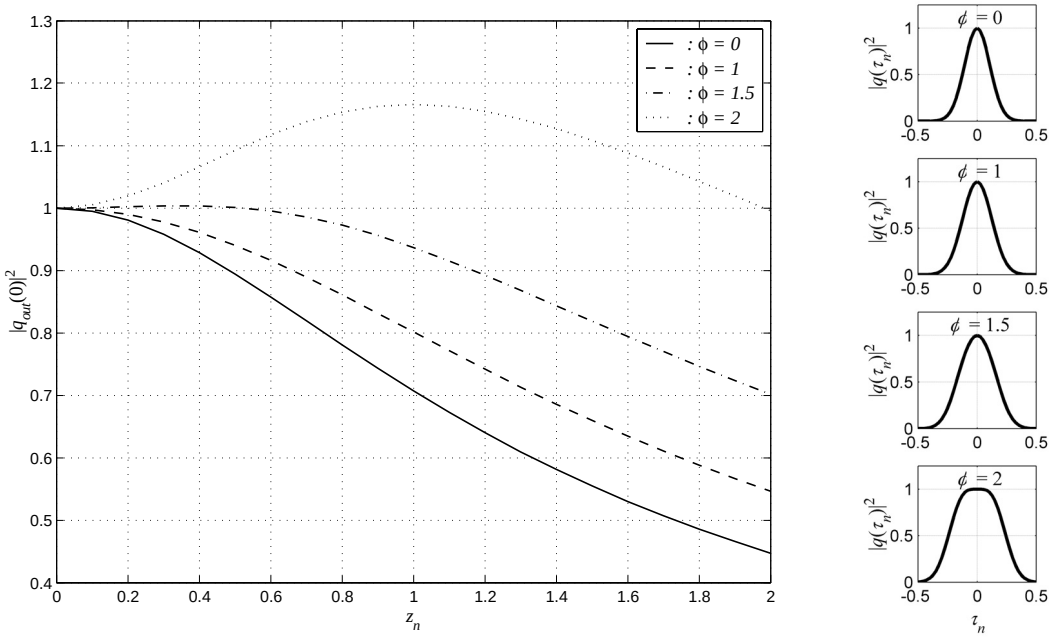

Fig. 4.5: Pulse peak power at the center $\left|q_{out}(0)\right|^2$ as a function of normalized transmission distance z_n at different values of $\phi = \delta / a_n$ when $P_0 = 1$. The right insets are the corresponding input pulse shapes $\left|q(\tau_n)\right|^2$ when $a_n = 0.15$.

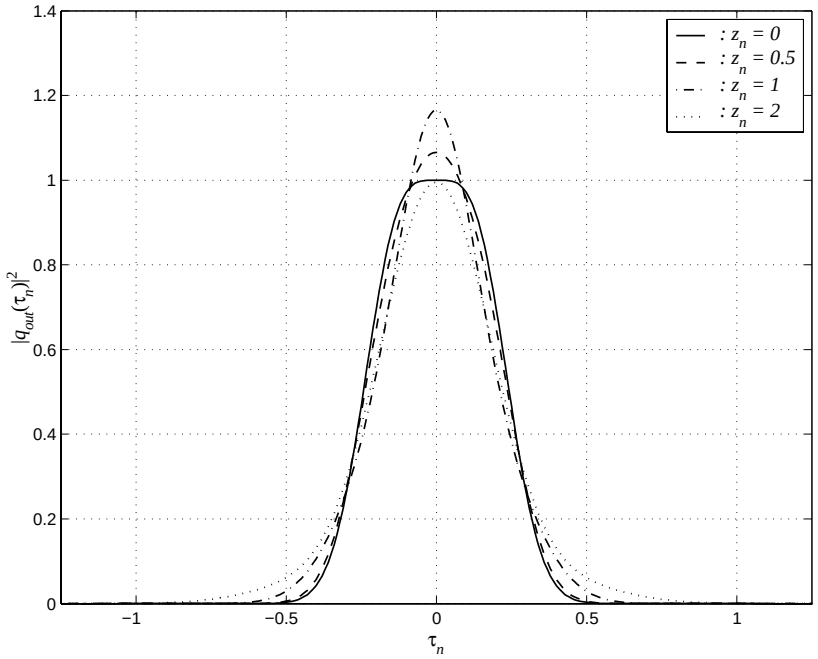

(a)

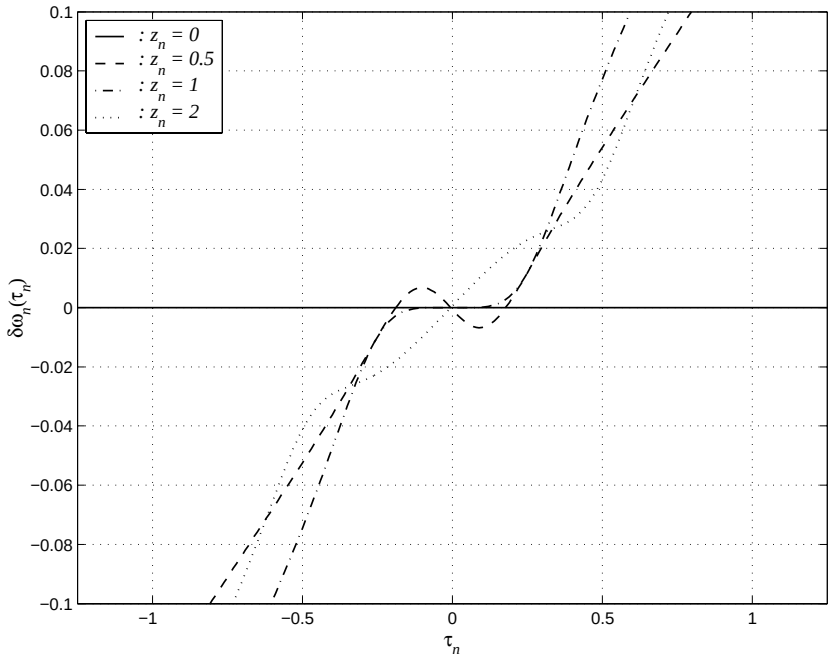

(b)

Fig. 4.6: (a) Snapshots of pulse evolution at different z_n as a function of normalized transmission distance z_n when $\phi = 2.0$, $a_n = 0.15$ and $\text{sgn}(\beta_2) = +1$. (b) Corresponding instantaneous frequency $\delta\omega_n(\tau_n)$ (frequency chirp) across the pulse.

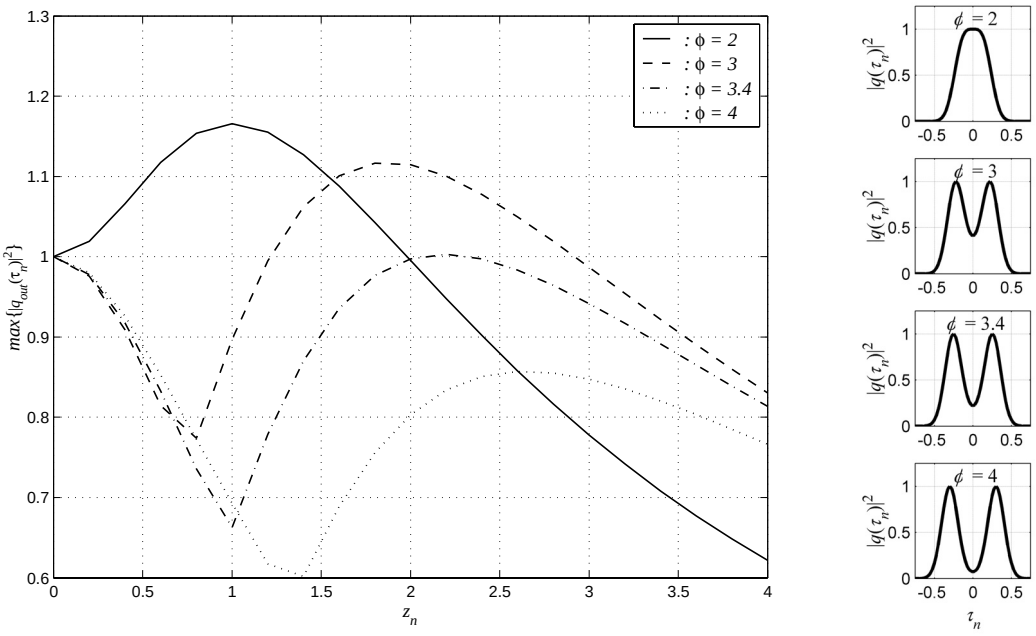

Fig. 4.7: Pulse peak power as a function of normalized transmission distance z_n at different values of $\phi = \delta / a_n$ when $P_0 = 1$. The right insets are the corresponding input pulse shapes $|q(\tau_n)|^2$ when $a_n = 0.15$.

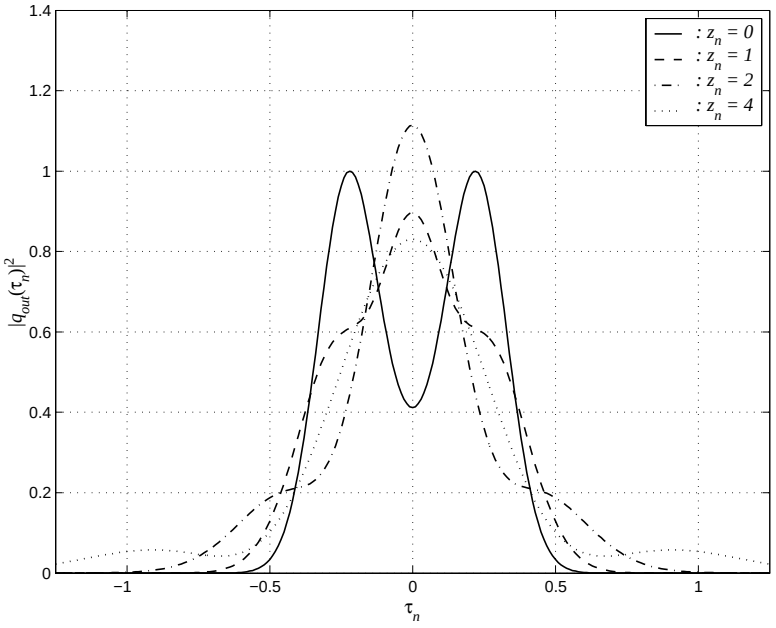

Fig. 4.8: Snapshots of pulse evolution at different z_n as a function of normalized transmission distance z_n when $\phi = 3.0$ and $a_n = 0.15$.

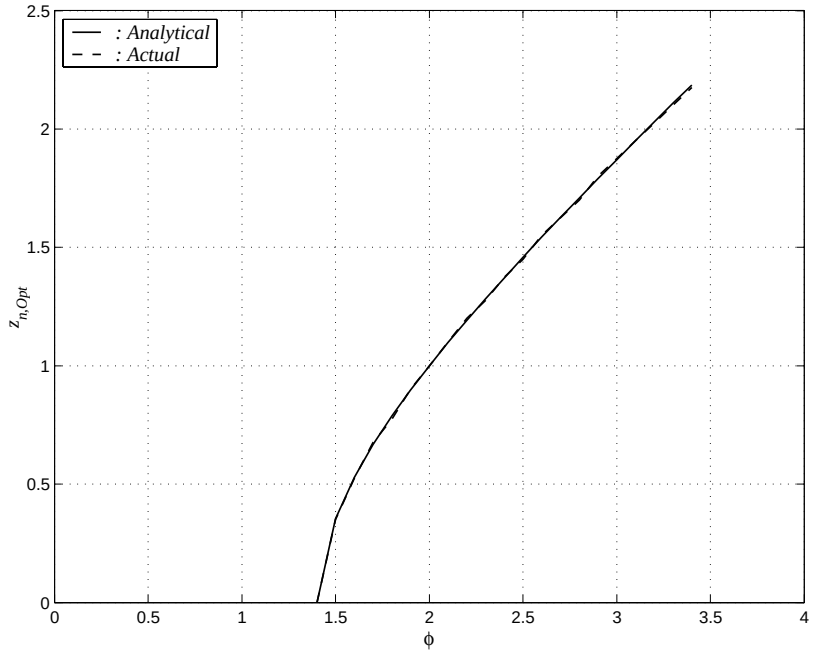

Fig. 4.9: Optimum transmission distance $z_{n,Opt}$ that yields strongest PIE as a function of ϕ. Note that the PIE occurs when $\sqrt{2} \le \phi \le 3.4$.

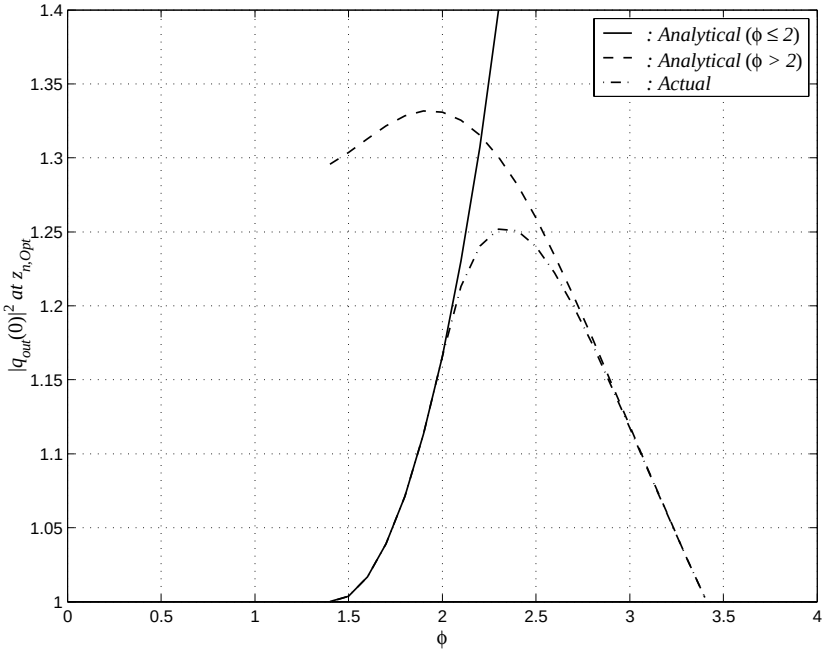

Fig. 4.10: Intensity at the center of the pulse $\left|q_{out}(0)\right|^2$ at $z_{n,Opt}$ as a function of ϕ.

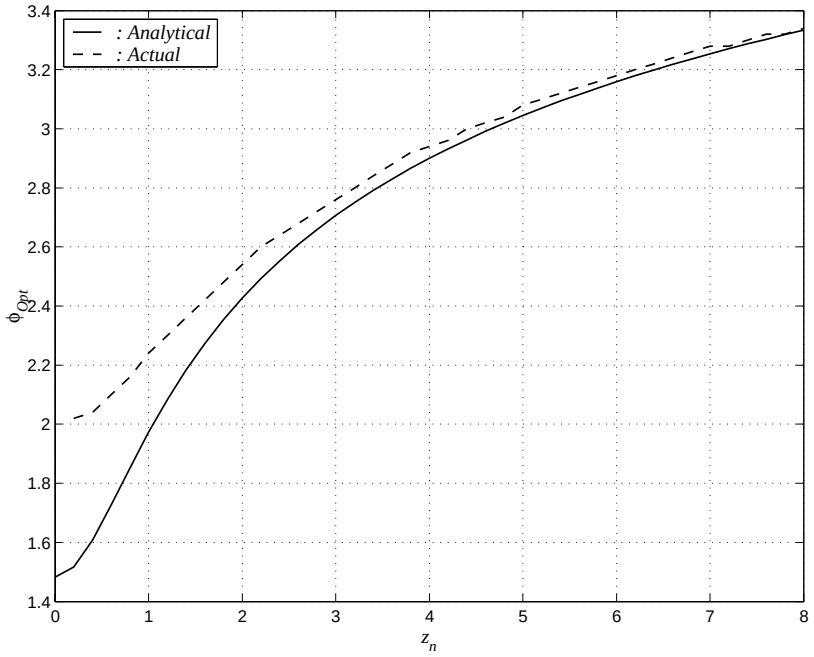

Fig. 4.11: Optimum value of ϕ that yields strongest PIE as a function of transmission distance z_n.

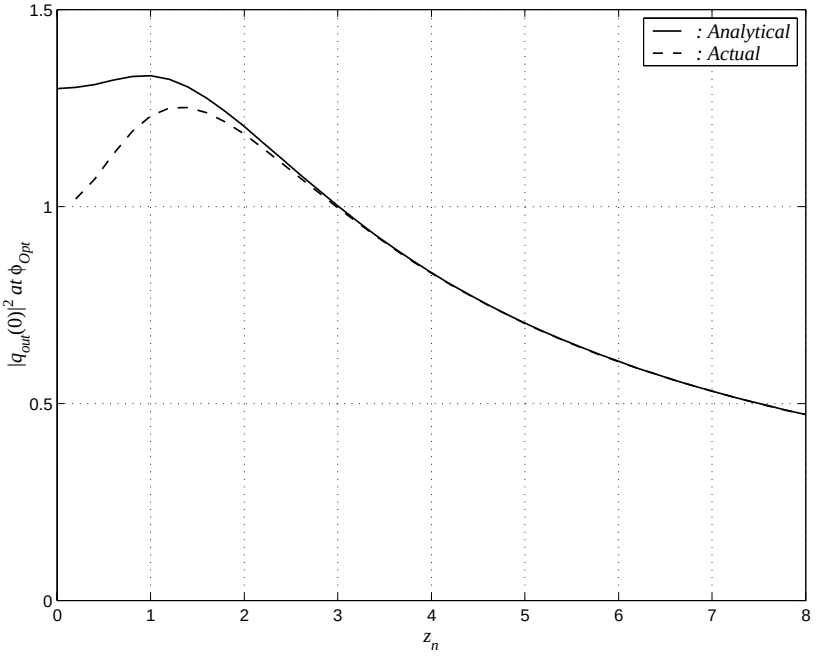

Fig. 4.12: Intensity at the center of the pulse $\left|q_{out}(0)\right|^2$ at ϕ_{Opt} as a function of z_n.

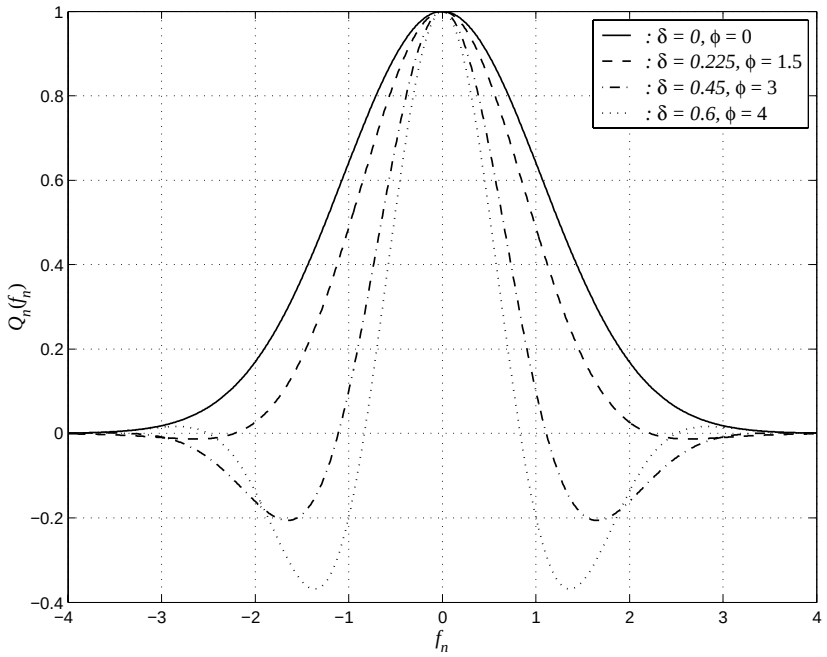

Fig. 4.13: Normalized Fourier transform of $q(\tau_n)$ at different values of ϕ when $a_n = 0.15$. Note that $Q_n(f_n)$ is normalized to have unit amplitude for ease of comparison.